Cosmological versus Intrinsic: The Correlation between Intensity and the Peak of the νF_ν Spectrum of Gamma Ray Bursts.

Nicole M. Lloyd[1], Vahé Petrosian[1], Robert S. Mallozzi[2]

[1] Center for Space Sciences and Astrophysics, Stanford University, [2] Dept. of Physics, University of Alabama in Huntsville.

ABSTRACT

We present results of correlation studies, examining the association between the peak of the νF_ν spectrum of gamma ray bursts, E_p, with the burst's energy fluence and photon peak flux. We discuss methods to account for data truncation in E_p and fluence or flux when performing the correlation analyses. However, because bursts near the detector threshold are not usually able to provide reliable spectral parameters, we focus on results for the brightest bursts in which we can better understand the selection effects relevant to E_p and burst strength. We find that there is a strong correlation between total fluence and E_p. We discuss these results in terms of both cosmological and intrinsic effects. In particular, we show that for realistic distributions of the burst parameters, cosmological expansion alone cannot account for the correlation between E_p and total fluence; the observed correlation is likely a result of an intrinsic relation between the burst rest-frame peak energy and the total radiated energy. We investigate this latter scenario in the context of synchrotron radiation from external and internal shock models of GRBs. We find that the internal shock model is consistent with our interpretation of the correlation, while the external shock model cannot easily explain this intrinsic relation between peak energy and burst radiated energy.

Subject headings: gamma rays: bursts – cosmology: miscellaneous.

1. Introduction

We now have confirmed redshift measurements to eight gamma-ray bursts (GRBs): 970228 (Djorgovski et al., 1999b), 970508 (Metzger et al., 1997, Bloom et al., 1998), 971214 (Kulkarni et al., 1998), 980613 (Djorgovski et al., 1999a), 980703 (Djorgovski et al., 1998), 990123 (Kelson et al., 1999, Hjorth et al. 1999), 990510 (Vreeswijk et al., 1999), 990712 (Galama et al., 1999). Although these redshifts have helped provide insight into the energetics of GRBs, they have not helped us gain knowledge on the cosmological distribution of GRBs as a whole. This is primarily because the "luminosity functions" of these bursts are broad, and mask any cosmological signature. Figures 1a and 1b show the Hubble diagram for GRBs and their afterglows with known redshifts (and for which the fluence and flux data is publicly available). There is no obvious Hubble relation

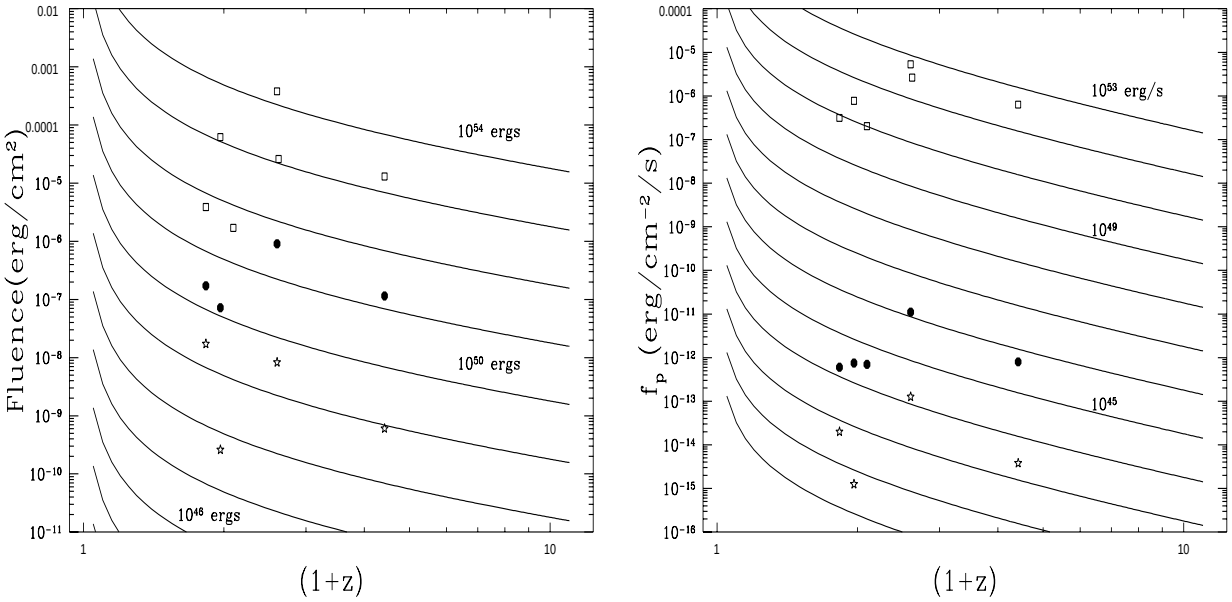

Fig. 1.— Hubble diagram for a) fluences (left panel) and b) peak fluxes (right panel) in the gamma-ray (squares), X-ray (filled circles) and optical (stars) energy ranges for GRBs with known redshifts. The solid lines are the expected relation in the Einstein-de Sitter cosmological model (with Hubble constant of 60 km/(s Mpc)) for indicated total radiated energy in (a) or average luminosity in (b). In Figure 1b, The X-ray fluxes are the values 8 hours after the burst, and the optical fluxes are either the peak or the earliest detection flux.

in any wavelength band, which suggests that we must continue to rely on statistical studies of GRBs to gain insight on their global distribution as well as the physical processes at the burst. Log$N$-Log$S$ studies have been extensively used to investigate the spatial distribution of GRBs, but one can easily show that any spatial distribution can fit the Log$N$-Log$S$ diagram, given some GRB luminosity function and a cosmological model (see e.g. Rutledge et al., 1995, Reichert and Mészáros, 1997, Mészáros and Mészáros, 1995, Hakkila et al., 1996). A more useful way to gain insight into the distribution and energetics of GRBs is to study correlations between various burst spectral and temporal properties. In this paper, we consider the correlation between a characteristic photon energy, for example the peak of the νF_ν spectrum, E_p, and fluence or flux. This can shed significant light on both the distributions and energetics of GRBs. For example, a burst that is further away will be weaker (assuming little luminosity evolution) and its spectrum will be redshifted; thus one would expect a positive correlation between a parameter such as E_p and fluence or flux, if cosmological effects were dominant. Intrinsic effects could either wash out or intensify such a correlation. Mallozzi et al. (1995) report the presence of a correlation between peak photon flux and E_p, consistent with the cosmological interpretation. However, the degree of the correlation can be affected by various detector selection biases. For example, because only the brightest bursts have adequate spectral data, many low intensity GRBs near the detection

threshold will be missing in the sample of bursts with spectral fits. This then will introduce a bias against bursts with peak counts near the threshold. Similarly, there may exist biases against high and low values of E_p (Lloyd and Petrosian, 1999; hereafter LP99). We investigate how the results are modified by the truncation of the sample due to such biases.

For reasons discussed below, we focus our study in particular on total fluence, F_{tot}, and E_p correlations for a sub-sample of brighter bursts. Our main goal is to determine the degree of correlation between these quantities, and investigate to what extent the correlation is due to cosmological redshift and to what extent it is a signature of an intrinsic relation between radiated power and spectral features. The former signature will be useful for investigations of spatial distributions and evolutionary processes associated with GRBs, while the latter will be important in constraining models of energy production and radiation processes in these sources. We find that there is a strong correlation between F_{tot} and E_p, and that this can be attributed to intrinsic effects, rather than to cosmological expansion or evolution of burst properties. We will briefly discuss the significance of these results for particular GRB models.

Getting an accurate handle on the amount of correlation between burst properties proves to be a challenging task, not only because we do not have redshift measurements for most bursts, but because we must account for the various biases and selection effects present in the GRB data. Because all detectors are sensitive over a finite energy range, and - in the case of BATSE - are subject to some trigger condition, selection effects are inevitable. For instance, as shown in Lee and Petrosian (1996) and LP99, the fluence, flux and E_p all suffer from some sort of data truncation imposed by the detector. As explained below, the detector is most likely to miss the high E_p bursts with low strength; a bias against high E_p bursts with low fluence or flux will have the effect of producing an apparent positive correlation in the data. Hence, a simple correlation analysis between raw values of E_p and burst strength without the consideration of the data truncation can lead to erroneous correlations. This will have an important effect on determining whether or not the correlations are intrinsic or due to cosmological redshift; hence, understanding the type and severity of truncation is necessary before attempting to perform correlation studies. In §2, we give a brief description of how we estimate the truncation imposed by the selection process, and determine how these truncations affect correlation studies. Further details are presented in the Appendix where we describe the non-parametric methods we use for the task at hand. In §3, we describe the data we use, and in §4, we present our results for the correlation of E_p with energy fluence and peak photon flux. In §5, we discuss the implications of these results in terms of cosmological and intrinsic effects. A summary and our conclusions are presented in §6.

2. Data Truncation

We need to understand how the detector thresholds affect the data analysis, and whether or not truncation effects are playing a role in the correlation analysis. Here, we focus on the BATSE

detector as an example. BATSE will trigger and begin recording data on a burst if the peak photon counts C_{max} in some finite time interval Δt (= 64, 256, or 1024 ms) and energy range ΔE (between E_1 and E_2; usually between 50 and 300 keV) is greater than C_{min}, determined by the background in the second brightest detector (out of eight detectors). This suggests that the detector efficiency is highest for longer duration bursts (see Lee and Petrosian, 1997), and for bursts with most of their photons in the range ΔE. As discussed in LP99, we can find the threshold(s) to any burst characteristic X measured by BATSE, utilizing the trigger condition. For each burst, we know X, C_{max}, and C_{min}. We can ask what is the possible range of values of X that this burst can have and still trigger the instrument. In general, X can have an upper limit u, a lower limit l, or both limits; $X \in T = [l, u]$.

For example, we can determine the detection threshold of the observed energy fluence F_{obs} (or peak flux f_p); in this case, there is only a lower limit $F_{obs,lim}$ (or $f_{p,lim}$). This threshold is obtained from the simple relation (Lee and Petrosian, 1996)

$$f_p/f_{p,lim} = F_{obs}/F_{obs,lim} = C_{max}/C_{min}. \tag{1}$$

The last equality is valid if the burst's spectrum does not change drastically throughout its duration. For other bursts characteristics, such a basic relation may not hold. For example, the break energy, E_B, or the peak energy, E_p, of the νF_ν spectrum of GRBs has both an upper and lower limit. The values of $E_{p,max}$ and $E_{p,min}$ are not related to C_{max}/C_{min} and E_p in a simple form as above, and thus we require a more complex procedure to determine their values. This was discussed in detail in LP99 and is summarized below.

To get a qualitative idea of how truncation could come into play, consider the following: We characterize the spectra of the bursts by four parameters: the low energy photon power law index, α, the high energy index, β, the break energy E_B (or $E_p = E_B(2+\alpha)/(\alpha-\beta)$ which is the peak of the νF_ν spectrum when $\alpha > -2$ and $\beta < -2$), and the normalization factor A. For an example, see equation (5) in §3, which is the parameterization used by Mallozzi et al. (1999, in preparation). Given a burst's spectrum $f_{\alpha,\beta,A}(E, E_p, t)$, the observed fluence is $F_{obs} = \int_0^T dt \int_{E_1}^{E_2} E F_{\alpha,\beta,A}(E, E_p, t) dE$ (where T is burst duration). The limiting value(s), $E_{p,lim}$('s), that E_p can take on and still trigger the BATSE instrument must satisfy the equation

$$F_{obs,lim} = \int_0^T dt \int_{E_1}^{E_2} E f_{\alpha,\beta,A}(E, E_{p,lim}, t) dE. \tag{2}$$

In general, there will be two values of $E_{p,lim}$ that satisfy this equation. To find these two solutions, we start with the observed value of E_p (for which the right side is equal to F_{obs}), and increase it (while keeping α, β, and the total fluence, $F_{tot} = \int_0^T \int_0^\infty E f_{\alpha,\beta,A}(E, E_p, t) dE$, equal to their determined values) until the above equality is reached - that is, until the observed fluence is brought to the level of the threshold. This value is the upper limit to E_p, $E_{p,max}$. We then decrease E_p until this equation is again satisfied; this gives the lower limit $E_{p,min}$. The choice of what is kept constant depends on the investigation at hand. We choose to keep the total fluence

constant because we are interested in the correlation between E_p and F_{tot} (for other types of investigations, one might keep, say, the normalization A constant).

However, in reality, BATSE triggers on counts, which is the convolution of the impinging photon flux with the detector response matrix, DRM. The DRM converts photons of a particular energy into detector "counts" over a range of energies. This allows for the possibility of photons from higher energies to spill over into the "observed" energy range. For example, given some C_{max} and C_{min}, and the detector response matrix, $DRM_{i,j}$ (where i and j index the energy bins for the incident photon flux and counts, respectively), the correct value for $E_{p,lim}$ is obtained from the following expressions:

$$C_{min,j} = \sum_i DRM_{i,j} * \int_o^T f_{\alpha,\beta,A'}(E_i, E_{p,lim}, t)\Delta E_i dt, \tag{3}$$

$$C_{min} = \sum_{Ch2+3,j} C_{min,j}. \tag{4}$$

where $A^{'}$ is the normalization in the spectrum appropriately adjusted to keep the total fluence constant. In other words, we have the incident photon spectrum characterized by α, β, E_p, and A in n energy bins of width ΔE indexed by i. To get the counts in m energy bins indexed by j, we multiply our photon model vector (of i components) by the detector response matrix - an $m \times n$ matrix, which converts photon flux into a count rate. We then sum over the energy bins for the count rate, corresponding to detector channels 2 and 3 ($\sim$ 50-300keV); this gives us the channel 2+3 count rate on which the detector triggers.

Equation (2), on the other hand, assumes that the DRM is strictly diagonal. Hence, the limits obtained based on this equation are only estimates of the true observational limits. Including the actual DRM would cause some spillover from channel 4, and contribute to the counts in channels 2 and 3. Preliminary analysis incorporating the DRM for a handful of bursts shows that including the precise detector response tends to increase the upper limit on E_p. In a future publication, we will present results which show how incorporating the actual shape of the DRM affects the limits of E_p. In this paper, we use a sample of bright bursts, which has a narrow distribution of E_p's and consequently requires a small correction due to instrumental biases (e.g. a delta function distribution requires zero correction; see also Brainerd, 1999). Thus, the truncations on E_p have little effect on the final results of our correlation studies for the chosen sample described in the next section. Nonetheless, we present results in which the effects of the limits on fluence and E_p are taken into account. In the Appendix, we present the results on how to perform correlation studies on data which suffer from truncation; these are based on new non-parametric techniques developed by Efron and Petrosian (1999). Once the truncation of the data is determined, we can then proceed to the investigation of correlations.

3. Data

Our sample consisted of a set of bursts from the 4B catalog (Paciesas et al., 1999) which have 16 channel CONT (continuous) data. Using these data, the bursts are fit to a Band Spectrum (1993). The spectrum is parameterized as follows:

$$f(E) = \begin{cases} A(E/E_B)^{\alpha}\exp[-(2+\alpha)(E/E_p)], & E < E_B \\ A(E/E_B)^{\beta}\exp[\beta-\alpha], & E > E_B \end{cases} \tag{5}$$

where A is units of ph/cm^2/s/keV. Note that for $\beta < -2$ and $\alpha > -2$, E_p is the maximum of $\nu F_\nu \propto E^2 f(E)$. Otherwise, νF_ν has no maximum and E_p is some characteristic photon energy. The parameter α is always greater than -2 in the fitting process so that νF_ν always converges for small ν; but β may exceed -2 which implies the peak of νF_ν must occur outside the range of detector sensitivity. The LP99 sample - based on four channel LAD data - contains a complete sample of bursts with known C_{max} and C_{min} values and therefore has a well defined truncation. Unfortunately the present 16 channel sample (containing a total of 653 bursts with acceptable fits for the fluence (time averaged) fits, and 655 bursts with acceptable fits for the peak flux fits) - although more reliable in the values of the spectral parameters - does not have a well defined selection criterion. Because the brightest bursts give the best fits, most bursts in this sample with a known C_{min} value have $C_{max}/C_{min} \gg 1$. These will obviously suffer less truncation effects than bursts with counts closer to the threshold; bursts with C_{max} near C_{lim} will have one or both $E_{p,lim}$'s near E_p and the truncation will be an important effect. In other words, the sample of bursts with reliable spectral fits is not complete to within well known limits, and the selection process most probably has introduced complicated truncations. Figures 2a and 2b show the sample of bursts which had spectral fits (circles), and those bursts in the catalog with known C_{max} and C_{min} values but no spectral fits (squares), in the $F_{tot} - F_{tot,lim}$ and $f_p - f_{p,lim}$ planes, respectively. As evident, there is not a clear indication of the nature of the selection process. Without exact knowledge of this selection criteria, we cannot account for data truncations properly or determine correlations accurately. To circumvent this situation, we choose the following sub-samples which have a better defined selection criterion. We truncate the available data parallel to the axes in Figure 2a and 2b, so that the above mentioned uncertainty is minimized. The truncation chosen here is a compromise which involves trying to get as large a sample (open circles) as possible, without too many missing bursts (black squares). That is, we attempt to minimize the bias without reducing the sample to an unreasonably small size. There are still a few bursts without spectral fits in this "complete" sample; however, we assume that these few bursts will not significantly alter the final result. For peak flux, the truncation was made at $f_p \geq 3.0$ ph/(cm^2 s), for the observed fluence (in the range 50-300 keV) we select a subsample with $F_{obs} \geq 10^{-6}$ ergs/cm^2, and for the summed fluence (summed over all four LAD channels (20keV$- \sim 1.5$MeV)) we select sources with $F_{sum} \geq 5 \times 10^{-6}$ ergs/cm^2.

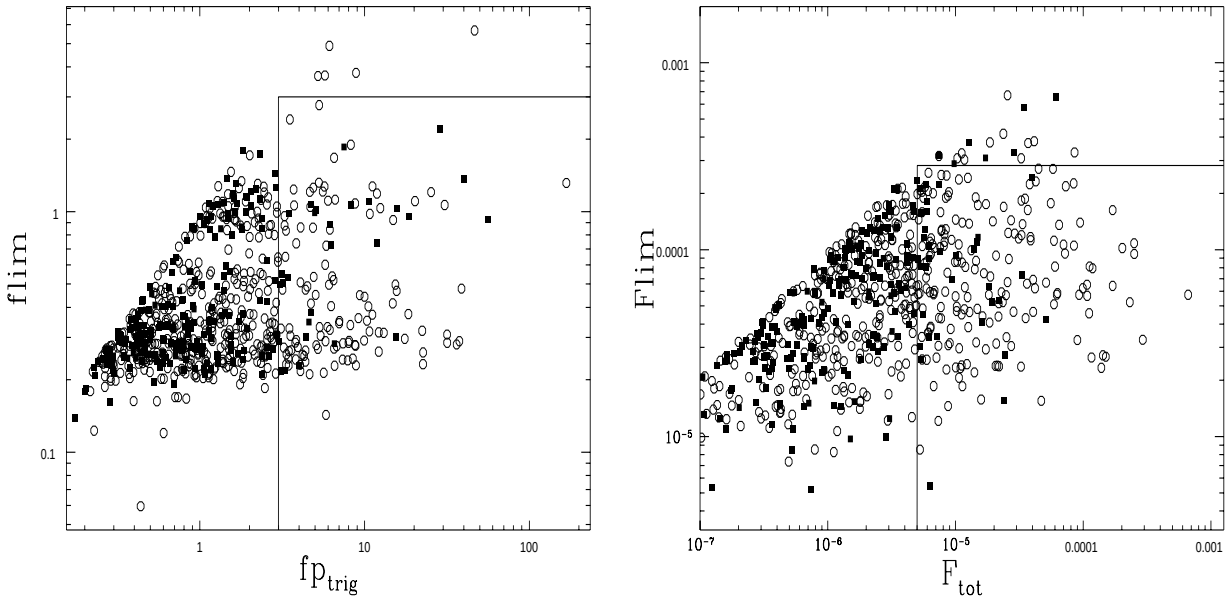

Fig. 2.— a) Peak flux, f_p vs. limiting flux, f_{lim} (left panel) and b) total fluence, F_{tot} vs. limiting fluence F_{lim} (right panel). The circles indicate the bursts with spectral fits, and the black squares mark those bursts in the catalog which do not have spectral fits. The box indicates our "truncated" sample, in which we attempt to get the most complete sample of bursts with spectral fits (i.e. fewest black squares in our sample), while still keeping a reasonable number of bursts for our statistical analysis.

4. Results

The results of our investigation of the correlation between peak flux and fluences with E_p are summarized in Figures 3a and 3b, and in Table 1. Note that F_{sum} is approximately equal to the total fluence of the burst, $F_{tot} = \int F(E)dE$ for E_p's in the energy range that we are dealing with. The fluences are correlated with the burst *average* E_p, while the peak photon flux is correlated with the value of E_p at the time of the peak. Figures 3a and 3b show binned values of E_p versus f_p and F_{tot}, respectively, for the whole sample without any consideration of completeness or detector bias (dotted histograms), as well as our more limited but complete sub-samples (solid histograms). The E_p versus f_p behavior for the whole sample is in agreement with the results reported by Mallozzi et al. (1998) on a slightly different sample . While there clearly is a significant correlation (particularly in the low end of the f_p distribution), it is not known how much of this is due to incompleteness of the data or other selection biases. The more complete sub-sample (solid histogram) shows very little correlation. The Kendell's τ test (see Appendix for further discussion) results shown in Table 1 are in agreement with the impressions from Figure 3a and quantify the differences between the whole sample and the sub-sample. The column labeled *raw result* shows

the significance of the correlation, τ, without accounting for truncation of the variables, while the *corrected result* uses the techniques described in the Appendix to account for these truncations. While the total sample shows τ values of $\sim 8\sigma$ for the correlation with f_p, the complete sample valid over a limited range of peak flux shows no significant ($< 3\sigma$) correlation. The correction for data truncations alter the results only slightly because of the narrowness of the E_p distribution, as mentioned above. It should be noted that the lever arm is small and most of the E_p - peak flux correlation *may* be contained in the low peak flux bursts; again, however, this is where the selection bias is the strongest so we cannot be certain that this is a real correlation between E_p and f_p.

TABLE 1

Simulation results for the case when truncation eliminates the correlation.

Correlation	raw result	corrected result
F_{obs} w/ E_p (whole)	(+) 5.1 σ	(+)8.0σ
F_{obs} w/ E_p (sub-smp)	(+) 5.6 σ	(+) 5.5σ
F_{sum} w/ E_p (whole)	(+) 7.5σ	(+)9.4σ
F_{sum} w/ E_p (sub-smp)	(+) 6.5σ	(+)5.8σ
$f_{p.trig}$ w/ E_p (whole)	(+) 7.9σ	(+)9.3σ
$f_{p.trig}$ w/ E_p (sub-smp)	(+) 2.5σ	(+)2.6σ

The behavior of the correlation between fluences and E_p is quite different. Although the significance of the correlation is large for the sample as a whole, Figure 3b shows that the functional dependence of the correlation is much stronger for high (solid histogram) rather than low valaues of the fluence. Again, because of the presence of many bursts without spectral fits in the whole sample, we do not know how accurate the functional form of the correlation in the low end of the fluence distribution is. In what follows, we shall use the truncated sub-sample of Figure 2b to search for cosmological signatures, because it shows a significant correlation and is more robust, due to our well defined truncation parallel to the axes in the $F_{tot} - F_{tot,lim}$ plane.

A least squares fit to $\log(E_p)$ - $\log(F_{tot})$ of the sub-sample (solid histogram) in Figure 3b gives a slope of 0.28 ± 0.04 (solid line). Our statistical methods presented in the Appendix give a similiar result: We define a new variable $E_p^{'} = E_p F_{tot}^{-\delta}$ and calculate the Kendell's τ statistic for the new variable $E_p^{'}$ and F_{tot} as a function of the parameter δ. Figure 4 shows this variation. The range of δ such that $|\tau| < 1$ determines the correct functional form form of the correlation. We find $\delta = 0.29 \pm 0.03$, meaning $E_p \propto F_{tot}^{0.29}$, in good agreement with the above least squares fit result.

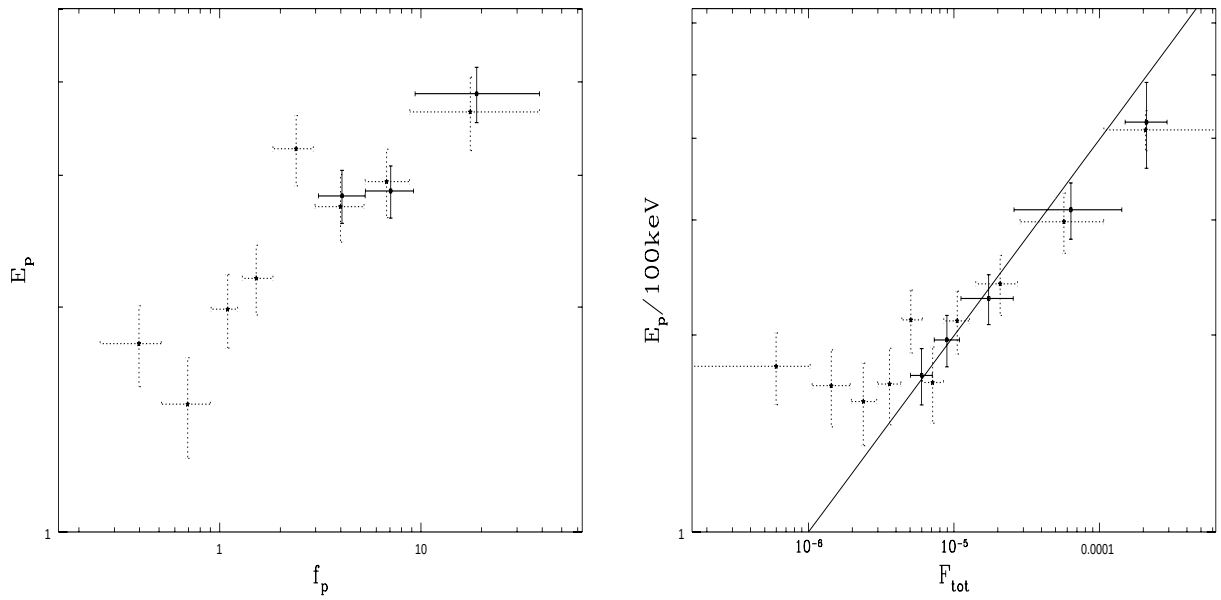

Fig. 3.— Average peak energy, $\overline{E_p}$ vs. a) peak flux, f_p (left panel) or b) total fluence, F_{tot} (right panel) for the whole (dashed histogram) and sub (solid histogram) spectral sample. Notice the flux shows a strong correlation at low values, but much less of a correlation for the brighter bursts. In the fluence case, the more complete sub-sample carries most of the correlation. The solid line is a least squares fit to the data which is in agreement with the functional form of the correlation we obtain from our statistical methods.

5. The Nature of the Observed Correlation

5.1. The Cosmological Correlation

A positive correlation between an observed burst strength (f_p or F) and E_p follows the trend expected from cosmological effects; bursts which are further away have lower intensity as well as a lower (redshifted) value of E_p. We now test to see if the observed correlations reported above can be attributed *fully* to these effects. We will focus particularly on the $F_{sum} \approx F_{tot}$ results, because - as mentioned above - it is our most robust result, and because the total fluence can be related to the total radiated energy and the redshift of the burst, without any need for the so-called K-correction or correction for duration bias (Lee and Petrosian, 1997); $F_{tot} = \mathcal{E}_{\rm rad}/(\Omega_b[d_{\mathcal{E}}(\Omega_i, z)]^2)$, where $\mathcal{E}_{\rm rad}$ is the total radiant energy (in the gamma-ray range), Ω_b is the average beaming solid angle, Ω_i denotes the cosmological model parameters, and $d_{\mathcal{E}}(\Omega_i, z) = d_L(\Omega_i, z)/\sqrt{(}1+z)$ with d_L as the usual bolometric luminosity distance. We also define E_{po} as the value of the peak of the νF_ν spectrum in the rest frame of the burst, so that $E_p = E_{po}/(1+z)$. For the task at hand, we need to specify a cosmological model, as well as the distribution function of redshift and intrinsic burst

parameters, $\Psi(E_p, \Omega_b, \mathcal{E}_{\rm rad}, z)$. Note that because the beaming angle enters always in conjunction with $\mathcal{E}_{\rm rad}$, we assume a delta function distribution of Ω_b so that it can be eliminated from the distribution function. This amounts to replacing $\mathcal{E}_{\rm rad}$ with $\mathcal{E}_{\rm rad}/\Omega_b$. We also assume that the intrinsic parameters $\mathcal{E}_{\rm rad}$ and E_{po} do not evolve with cosmic time and are not correlated. These assumptions mean that the multivariate distribution function becomes separable;

$$\Psi(E_{po}, \Omega_b, \mathcal{E}_{\rm rad}, z) = \phi(\mathcal{E}_{\rm rad})\zeta(E_{po})\rho(z). \tag{6}$$

If now we change variables from $\mathcal{E}_{\rm rad}$ to F_{tot} and E_{po} to E_p, we get the joint distribution of observed E_p and F_{tot} as

$$\frac{d^2N(E_p, F_{tot})}{dE_p dF_{tot}} = \int_0^\infty dz (dV/dz)\rho(z)[d_{\mathcal{E}}(\Omega_i, z)]^2 \phi(F_{tot}[d_{\mathcal{E}}(\Omega_i, z)]^2)(1+z)\zeta(E_p(1+z)), \tag{7}$$

where dV/dz is the differential of the co-moving volume up to z. From this we can compute the individual distributions, and average value of E_p as a function of F_{tot}. For example,

$$\overline{E_p(F_{tot})} = \frac{\int dE_p E_p [d^2N(E_p, F_{tot})/dE_p dF_{tot}]}{dN(F_{tot})/dF_{tot}}, \tag{8}$$

where the differential source count in terms of fluence is

$$dN(F_{tot})/dF_{tot} = \int dE_p [d^2N(E_p, F_{tot})/dE_p dF_{tot}]. \tag{9}$$

[In an analogous manner, we can find the differential distribution of E_p and the average value $\overline{F_{tot}(E_p)}$.] We now have an expression for average observed E_p as a function of the observed total fluence. Implicit in this expression is the cosmological contribution to the correlation between $\overline{E_p}$ and F_{tot}. To see if this is the form of the correlation observed in the data, we carry out the following tests: We assume various plausible models for the functions ζ, ϕ, and ρ, and compute the expected cosmological relation $\overline{E_p(F_{tot})}$. We then remove this correlation from the data by the transformation $E_p^{'} = E_p/\overline{E_p(F_{tot})}$, and see if we are left with any correlation between the observed F_{tot} and $E_p^{'}$ distributions. Only if none remains (i.e. $|\tau| < 1$, where - again - τ indicates the significance of the correlation between F_{tot} and E_p), then we can attribute the correlation between F_{tot} and E_p to cosmological effects alone.

Assuming no intrinsic correlation between $\mathcal{E}_{\rm rad}$ and E_{po} as in equation (6), we try several models for the functions ϕ, ζ, and ρ. We assume that ζ is a Gaussian with a mean value for E_{po} of Q and a dispersion σ_Q, ϕ is either a delta function (standard candle) or a power law in the radiated energy, and ρ is either a constant or follows the star formation rate. We present results for the Einstein de-Sitter cosmological model, and adopt a Hubble constant of 60 km s^{-1}Mpc^{-1};

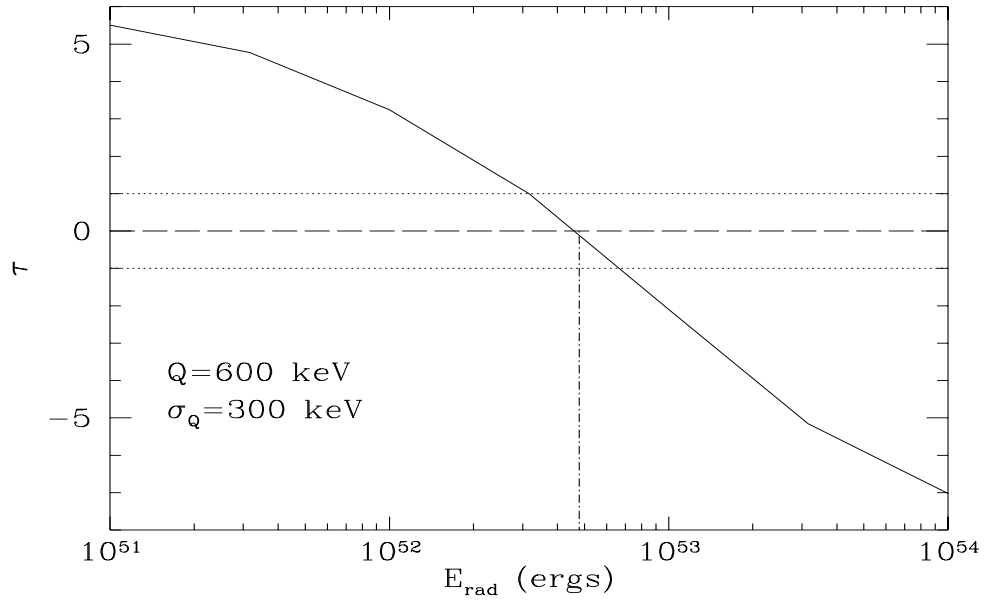

Fig. 4.— Significance of the correlation, τ, vs. radiated energy, $\mathcal{E}_{\rm rad}$, for the model given in case 1 of §5.1 in the text. Here, we find that the correlation is removed for a standard candle energy of 5×10^{52} erg. This result is independent of the GRB density distribution.

however, we find the quantitative results are insensitive to the cosmological model we choose. For example, a vacuum dominated universe with $\Omega_{\rm matter} = 0$ and $\Omega_\Lambda = 1$ (where Λ is the cosmological constant), leads us to almost exactly the same results as a matter dominated Einstein-de Sitter universe with $\Omega_{\rm matter} = 1$, $\Omega_\Lambda = 0$.

Our general conclusion is that, for the more plausible values of the parameters for this set of distributions, most of the observed correlation cannot be attributed to cosmological effects alone, and must be intrinsic to the emission mechanism or produced by additional evolution of the sources. We give two examples below:

1) For a *standard candle radiated energy*, $\mathcal{E}_*$, i.e. $\phi = \delta(\mathcal{E}_{\rm rad} - \mathcal{E}_*)$, our expression for the average E_p as a function of total fluence becomes:

$$\overline{E_p(F_{tot})} = \frac{\int dE_p E_p \exp[-(E_p Z_o - Q)^2 \sigma_Q^2]}{\int dE_p \exp[-(E_p Z_o - Q)^2 / \sigma_Q^2]} \tag{10}$$

where $Z_o^{1/2} = 1 + ((H_o/2c)^2 \mathcal{E}_* / F_{tot})^{1/2}$. Note that because of the delta function in energy, we are able to eliminate the redshift integral (a single redshift is picked out), and the expression becomes independent of the rate density evolution. In Figure 4, we plot τ as a function of $\mathcal{E}_*$. Here we see that the correlation *can* be removed ($|\tau| < 1$) for $\mathcal{E}_* = (5 \pm 2) \times 10^{52}$ ergs (this result is fairly insensitive to the value of Q and σ_Q of the E_{po} distribution). However, we know from the bursts

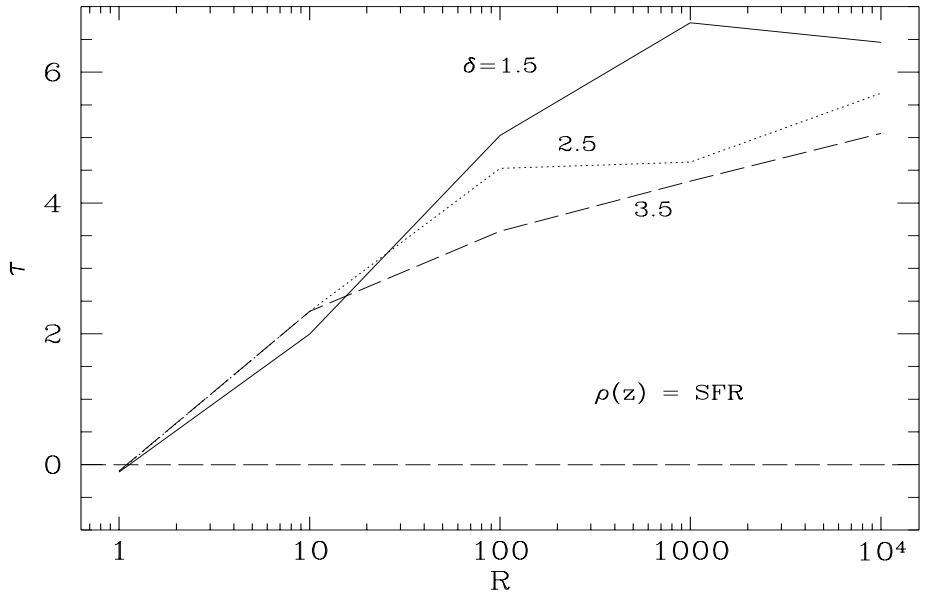

Fig. 5.— Significance of the correlation, τ, vs. $R \equiv \mathcal{E}_{\rm max}/\mathcal{E}_{\rm min}$, for the model in case 2 of §5.1 in the text. The variables $\mathcal{E}_{\rm max}$ and $\mathcal{E}_{\rm min}$ are the upper and lower cutoffs to the burst power law luminosity function, respectively. Here, we have chosen $\sqrt{\mathcal{E}_{\rm max}\mathcal{E}_{\rm min}} = 5\times10^{52}$, so that when $R \to 1$, we recover our result in Figure 4 above. The curves are shown for three different values for the luminosity function index β, and for a density following the star formation rate. The results are qualitatively similiar for a constant GRB density, or the intermediate SFR given in the text.

with measured redshifts (e.g., see Figure 1) that a delta function in burst radiated energy is not a good approximation. Hence we try a more realistic model for the distribution of burst parameters.

2) Here, we choose a *power law distribution in the radiated energy*, $\phi = \mathcal{E}_{\rm rad}^{-\delta}$, with upper and lower cutoff $\mathcal{E}_{\rm max}$ and $\mathcal{E}_{\rm min}$. Again, the expression for $\overline{E_p(F_{tot})}$ is obtained from equations (8) and (9) with

$$d^2N(E_p,F_{tot})/dE_p dF_{tot} = \int_{z_{min}}^{z^{max}} dz \frac{dV}{dz}(1+z)[d_{\mathcal{E}}(\Omega_i,z)]^{2-2\beta}\rho(z)\exp[-(E_p(1+z)-Q)^2\sigma_Q^2] \quad (11)$$

where $(1+z_{min})^{1/2} = 1+((H_o/2c)^2\mathcal{E}_{\rm min}/F_{tot})^{1/2}$, and $(1+z_{max})^{1/2} = 1+((H_o/2c)^2\mathcal{E}_{\rm max}/F_{tot})^{1/2}$. We test both $\rho(z)$ following the star formation rate and $\rho(z)$ as a constant. We use two different star formation rates (SFRs). In the first, based on results from Madau et al. (1998), the SFR peaks at $z \sim 2$, and then decreases slowly for high z. In the second model, based on recent results from SCUBA (Hughes et al., 1998, Sanders, 1999), the SFR remains approximately constant for $z > 2$. [Note this latter parameterization of the SFR falls in between the Madau parameterization and the constant rate case.] Our results from all three models for the co-moving

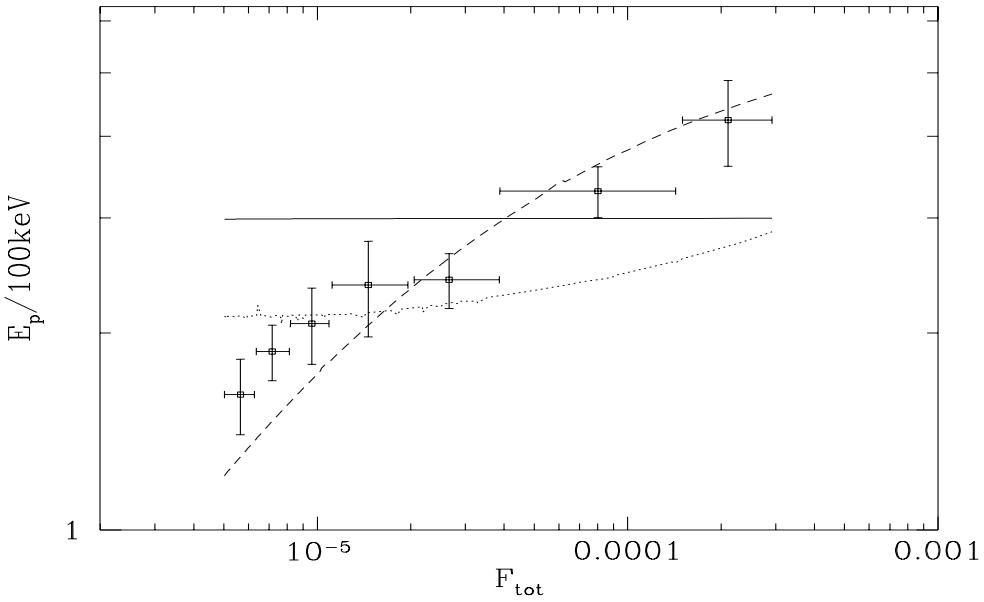

Fig. 6.— Total fluence, F_{tot}, vs. average peak energy, E_p. The crosses mark the data points binned (every 20) in fluence. The curves correspond to the theoretical functions computed in examples 1 and 2 in §5.1 of the text. The dashed curve is the case of a constant radiated energy, $\mathcal{E}_*$. The dotted curve is for a power law luminosity function, with $R = 10^4$, and a constant GRB density. The solid curve is the same, but with GRBs following the Madau star formation rate. Notice the latter two functions cannot account for the observed correlation as shown in Figure 5 above. The dashed curve shows the model in case 1 (standard candle energy) can account for the correlation, as we see in Figure 4.

rate density are quantitatively similar (note in the following figures, "SFR" will refer to the Madau parameterization). Figure 5 plots τ vs. $R \equiv \mathcal{E}_{\rm max}/\mathcal{E}_{\rm min}$ for a density following the SFR. Here we have chosen $\sqrt{\mathcal{E}_{\rm min}\mathcal{E}_{\rm max}} = 5 \times 10^{52}$ erg; note that when $\mathcal{E}_{\rm max}/\mathcal{E}_{\rm min} = 1$ or if $\delta \gg 1$, we get back the delta function case above, where the correlation is removed. In general, for a broader, more realistic "luminosity function", the correlation due cosmological expansion is smeared out and becomes too weak to explain the strong observed correlation. We find a similar result for the case when $\rho =$ constant or the intermediate SFR.

Another way to view these results is shown in Figure 6. Here, we have plotted the theoretical curves $\overline{E_p(F_{tot})}$ on top of the data for three of the cases mentioned above. The curve from case 1 (in which the luminosity function is a delta function (dashed curve)) follows the data fairly well, while the curves from the second, more realistic cases (in which the luminosity function is a power law and the density is either constant (dotted curve) or follows the SFR (solid curve)) are too flat; the cosmological correlation is washed out by the dispersion in the radiated energy. The natural

interpretation in this case is that the observed correlation between F_{tot} and E_p is either caused by the cosmological evolution of one or more of the parameters or is due to an intrinsic correlation between E_{po} and $\mathcal{E}_{\rm rad}$.

5.2. Evolutionary Effects

If $\mathcal{E}_{\rm rad}$ and/or E_{po} depend on redshift, we can not separate our variables as we have done in equation (6). In that case, we expect a different $E_p - F_{tot}$ correlation than in the case when the intrinsic variables are separable from redshift (not evolving). For example, if the luminosity function evolved such that a characteristic $\mathcal{E}_{\rm rad}$ *decreased (increased)* with increasing redshift, then we would see a *stronger (weaker)* correlation due to cosmological effects than presented in the examples given above. This type of evolution must be explained by models of the progenitors of GRBs, and may be difficult to achieve. Likewise, if the bursts' intrinsic peak energies, E_{po}, were on average *lower (higher)* in the past, then we would see a *stronger (weaker)* correlation between E_p and F_{tot} than if there were no evolution of E_{po}. We might expect some evolution if E_{po} depends strongly on the conditions of the circumburst medium (e.g., in the external shock model discussed below), *and* if the medium itself evolved strongly with redshift. To account for the strong correlation we see in the data, the circumburst medium would have to become more dense with decreasing redshift. However, we might expect that the progenitors of GRBs have approximately the same type of environmental conditions; for example, if bursts are a result of the death of a very massive star and occur in star forming regions as these models predict, then we expect the circumburst densities to be about same. However, we know too little about the conditions of the environment around the progenitor of GRBs to say anything definite about this possibility.

5.3. Intrinsic Correlation

Perhaps a more likely scenario is that the intrinsic variables $\mathcal{E}_{\rm rad}$ and E_{po} are correlated. For instance, the physics of the burst emission may lead to a case in which bursts with more total energy radiate at higher peak energies.

To examine this possibility more closely, we repeat the procedure described in §5.1 assuming a power law parametric form for the intrinsic correlation between Q, the mean of the E_{po} distribution, and $\mathcal{E}_{\rm rad}$; $Q \propto \mathcal{E}_{\rm rad}^{\eta}$. We vary η until the correlation between E_p and F_{tot} is removed ($|\tau| < 1$). For a model as in case 2 where $\phi = \mathcal{E}_{\rm rad}^{-\delta}$, $\mathcal{E}_{\rm min}/\mathcal{E}_{\rm max} = 10^{2.5}$ (a somewhat broad luminosity function, within the range of the dispersion shown in Figure 1b), $\delta = 2.5$, and $\rho =$ SFR, we find that we can remove the observed correlation if $Q \propto \mathcal{E}_{\rm rad}^{0.47\pm0.08}$. Similarly, in the same

model except with a *constant* density, we find that we can remove the correlation in the data if $Q \sim \mathcal{E}_{\rm rad}^{0.62\pm0.1}$. [Clearly an intermediate exponent is expected for the SFR model that is constant for $z > 2$.] These results can be used to test models of GRB emission, most of which predict some sort of relation between these quantities.

For example, if the emission can be explained by optically thin synchrotron radiation with a power law distribution of electrons, then E_{po} in the cosmic co-moving frame of the burst can be written (see, e.g., Pacholczyk, 1970)

$$E_{po} = \frac{3he\gamma_m^2 B_\perp \Gamma}{4\pi mc} \tag{12}$$

where γ_m (which we assume is $\gg 1$) is the lower cutoff to the electron power law distribution, $N(\gamma) = N_o\gamma^{-p}$, Γ is the bulk Lorentz factor of the emitting source, and $B_\perp$ is the perpendicular component of the magnetic field. To a very rough approximation, we may estimate the radiated energy of the GRB as the duration T times the total power emitted per electron, integrated over the initial electron energy distribution:

$$\mathcal{E}_{\rm rad} \propto T\Gamma^2 N_o \int_{\gamma_m}^{\infty} \gamma^{-p} d\gamma [\frac{4\sigma_T c B^2 \gamma^2}{24\pi}] \propto T N_o B^2 \Gamma^2 \gamma_m^{3-p} \tag{13}$$

where σ_T is the Thomson cross section, and the expression in brackets is the total power radiated by an electron of Lorentz factor γ. The last proportionality comes from performing the integration for $p > 3$. If, for example, in a very simple model where γ_m, T, and N_o were constant from burst to burst or independent of $B_\perp$ and Γ, then we would find that $E_{po} \propto \mathcal{E}_{\rm rad}^{1/2}$, consistent with our results above. However, this ignores many of the subtleties of the GRB emission. More detailed models which include information about the progenitor and environments around the GRB will predict different relationships among the parameters B, T, N_o, Γ, and γ_{min} and - in particular - relate them to the total radiated energy of the burst in a more precise way than done above.

It is generally agreed that the GRB radiation is produced by the action of a blast wave with two basic independent parameters - the total energy, $\mathcal{E}_{\rm tot}$, and the bulk Lorentz factor, Γ. However, whether the gamma-ray emission occurs in external or internal shocks is a matter of dispute. In the *the external blast wave model* (see, e.g., Dermer, Chiang, and Boettcher, 1998, and reference cited therein), both γ_m and B will be proportional to the bulk Lorentz factor so that $E_{po} \propto \Gamma^4$. The proportionality constant depends on details such as the circumburst density, shock compression ratio, the fraction of energy that goes into the magnetic field or relativistic electrons, but *not* on the other basic parameter of the blast wave - namely, the total energy $\mathcal{E}_{\rm tot}$. On the other hand, the radiated energy $\mathcal{E}_{\rm rad}$ is assumed to be proportional to $\mathcal{E}_{\rm tot}$ with the proportionality constant fairly independent of Γ. Thus, we expect no observed correlation between E_p and F_{tot}, except for the weak cosmological contribution. The strong correlation we see in the data is therefore in disagreement with this model.

The above relations are more complicated in an *internal shock scenario* (Rees & Mészáros, 1994, Sari & Piran, 1997), because of the presence of additional parameters such as the Lorentz

factors of the shocked shells, the shells initial separations, the width of the complex of shells, etc. (see Piran, 1999 for a review). From equations (53), (83), and (84) of Piran, one can show that $E_{po} \propto \mathcal{E}_{\rm tot}^{1/2} \Gamma^{-2} \gamma_{int}^{5/2}$, where γ_{int} is the Lorentz factor of the internal shock. If again we assume that $\mathcal{E}_{\rm rad} \propto \mathcal{E}_{\rm tot}$, with proportionality constant independent of γ_{int}, Γ, etc., and that $\mathcal{E}_{\rm rad}$ and Γ (or γ_{int}) are independent parameters of the model, then we find $E_{po} \propto \mathcal{E}_{\rm rad}^{1/2}$. This is consistent with the results presented above; thus, we may conclude that the analyses presented here favor the internal shock model.

6. Conclusion

From the few bursts with measured redshifts, it is clear that GRBs have a broad luminosity function (Figures 1a and 1b); as a result, direct detection of cosmological signatures is difficult, and requires a large number of GRBs with known redshifts. Hence, we must continue to rely on statistical studies of GRB properties to look for such signatures. In this paper we analyze the correlation between observed burst strengths (peak flux or fluence) and photon spectrum characterized by the peak energy, E_p, of the νF_ν spectrum. Some or all of this correlation could be due to the combined effects of spectral redshift and source dimming with distance. There has been some evidence for such a correlation.

The data we use for these purposes come from the BATSE detector on CGRO. Our spectral parameters - in particular E_p - are obtained from fits to 16 channel CONT data; the fluences and peak fluxes are taken from the 4B catalog (Paciesas et al., 1999). In order to get an accurate measure of the correlations present in the data, we must be sure to account for all types of selection effects present. In LP99, we discuss the observational thresholds on both E_p and measures of burst intensity and how this might affect correlation studies, and in the Appendix of this paper we review the non-parametric techniques that we use to account for data truncations. However, in addition to these truncation effects, there are subtle selection effects specific to bursts with spectral data. In particular, the bursts near the instrument's threshold generally do not have sufficient data for a reliable spectral fit. Hence, the existing samples are missing many bursts with peak counts C_{max} near the threshold C_{min}. It is difficult to quantify what the effect of this will be on our correlation studies. To circumvent these additional selection biases, we selected a sub-sample of bright bursts which are fairly complete in terms of C_{max}/C_{min}. This sample has a well defined selection criterion, and hence the results we obtain from this sample are more robust and reliable. Applying our methods, we find the following results:

a) We find a strong correlation between peak flux and E_p for the whole spectral sample, in agreement with earlier results reported by Mallozzi et al. (1995, 1998). However, the sub-sample of bright bursts selected in Figure 2a shows only a marginal correlation between peak flux and E_p. On the other hand, we find significant correlations between the burst fluence and E_p for both

the whole sample as well as the sub-sample shown in Figure 2b. The sub-sample, however, shows a much steeper functional dependence than the whole sample (Figure 3b). In our subsequent analysis, we focus on the total fluence, F_{tot}, and E_p correlation in the sub-sample, because the truncation effects in this sub-sample are better understood, and the investigation of the cosmological interpretation is simplest in this case.

b) We quantitatively test to see if our $F_{tot} - E_p$ correlation can be attributed to cosmological effects alone. This, of course, depends on the cosmological model, intrinsic distributions of the burst parameters, as well as the co-moving rate density of GRBs. We start with the assumption that there are no correlations between intrinsic burst parameters, and that cosmological evolution of these parameters is minimal. We present results for an Einstein-de Sitter cosmological model, although similar conclusions are reached in other reasonable cosmological models we have tested.

c) We find that the observed correlation can be explained by cosmological expansion alone if the total radiated energy (in the gamma ray range) is constant (standard candle assumption). This result is independent of the GRB rate density, and is fairly insensitive to the distribution of the other intrinsic burst parameters. However, as mentioned above, a narrow distribution of radiated energy or luminosity is inconsistent with the data from bursts with observed redshifts.

d) For a more plausible, broad luminosity function (e.g., a power law distribution $\phi(\mathcal{E}_{\rm rad}) \propto \mathcal{E}_{\rm rad}^{-\delta}$), we find that neither for a constant co-moving rate density nor for rates proportional to the star formation rate, can the correlation be solely attributed to cosmological expansion. The expected correlation is essentially "washed out" by the broad luminosity function.

e) This implies either the presence of strong evolutionary effects, or an intrinsic correlation between GRB properties. We find that the first possibility is less likely than the second. We conclude, then, that the observed correlation between F_{tot} and E_p must be primarily due to an intrinsic correlation between the total radiated energy, $\mathcal{E}_{\rm rad}$, and the rest frame peak energy, E_{po}. Using our methods, we find that for broad luminosity functions, we can explain the observations if the intrinsic correlation obeys a power law, $E_{po} \propto \mathcal{E}_{\rm rad}^{\eta}$, with $0.7 < \eta < 0.4$, depending on the form of the co-moving rate density.

f) This kind of correlation seems to be a natural consequence of optically thin synchrotron emission by a power law distribution of electrons with Lorentz factors greater than some minimum cutoff, γ_m. Using the results from a detailed modeling of the emission in an external or internal shock model, we find that the internal shock model can explain the strong intrinsic correlation more simply.

These results are based on a sub-sample of bursts with a limited range of intensity. This range can be expanded and the results can be put on more solid footing by using the complete sample of GRBs observed by BATSE. This, however, requires a better understanding of the selection effects involved in the entire process of detection and spectral fitting. These questions will be explored in more detail in a future publication.

We would like to thank Rob Preece and Ralph Wijers for useful discussions. This research was supported by NASA grant NAG5-7874.

A. Appendix

A.1. Estimating the True Correlation of Truncated Data

We want to examine the correlation of E_p with some measure of burst intensity - for example, the total fluence, F_{tot}. However, we need to account for the fact that E_p has both an upper and lower limit, $E_{p,max}$ and $E_{p,min}$, and that F_{tot} has a lower limit, F_{lim}, to get an accurate estimate of the true correlation. We can use the τ statistic to test the degree of correlation.

$$\tau = [\frac{\text{positive comparisons} - \text{negative comparisons}}{\text{total comparisons}}] \times \sigma^{-1} \tag{A1}$$

A positive comparison corresponds to (a) $E_{p,i} > E_{p,j}$ and $F_{tot,i} > F_{tot,j}$, *or* (b) $E_{p,i} < E_{p,j}$ and $F_{tot,i} < F_{tot,j}$. A negative comparison corresponds to (a) $E_{p,i} > E_{p,j}$ and $F_{tot,i} < F_{tot,j}$ *or* (b) $E_{p,i} < E_{p,j}$ and $F_{tot,i} > F_{tot,j}$. The variable σ is the standard deviation of the numerator; in the usual Kendell's τ test with no truncation, $\sigma = [(4N + 10)/(9N(N - 1))]^{1/2}$, where N is the total number of data points. Note that when variables suffer from truncation, a point can be compared with another only if it could have been detected in the limiting range of the other, and vice versa; that is, two points can be compared when they are in the limits of one another - $E_{p,i} \in [E_{p,max,j}, E_{p,min,j}]$, $E_{p,j} \in [E_{p,max,i}, E_{p,min,i}]$, $F_{tot,i} > F_{lim,j}$, *and* $F_{tot,j} > F_{lim,i}$.

Once we get a value for the numerator in equation(A1) above, which estimates the degree of correlation between E_p and F_{tot}, we must determine the significance of the correlation by finding the value of σ. For the case when variables are truncated, we cannot simply use the formula for the usual Kendell's τ test given above. To find σ, we draw N (where N $\sim$ 100 or more) bootstrap vectors from the observed distribution of, for example E_p, and compute the comparison statistic (numerator in equation (A1)) for these vectors (Efron and Petrosian, 1999). From the distribution of these comparison statistics, we can compute a mean and standard deviation. This gives an estimate of the significance of the correlation (i.e. what we have defined as τ above). For instance, $\tau = 0$ implies no correlation while $\tau = 1$ implies a 1σ correlation. We can then determine true correlations between parameters which suffer from truncation. Once we have an estimate of the degree of correlation, we can probe the functional dependence of the correlation. This is described in more detail below.

A.2. Recovering the Original Degree of Correlation

We perform simulations to demonstrate how well this method can recover the amount of correlation present in the original (parent) distribution, given that we observe a truncated sample. We simulate the spectra of 1000 bursts. The parameter E_p and the normalization A are taken from an assumed distribution, while the indices α and β are held constant. Note that we are not attempting to reproduce the actual distributions of the burst parameters here, but merely want to illustrate how well this method can recover the parent correlation given some truncation on the data. Of course, the validity of the method is independent of the choice of burst parameters we use - we present those simulations in which the truncation has the most dramatic effect. From knowledge of the spectral parameters, we can calculate the burst total fluence, F_{tot}. We then can immediately compute the degree of correlation between E_p and F_{tot}, present in the in the *original* sample. We then simulate the limiting fluence F_{lim} of each burst, and ask: How many bursts have fluence above their threshold, F_{lim}? Only a fraction of bursts (in our simulations, typically half) will make this cut. This is our *observed* sample.

We then apply the methods described above to our *observed* sample to determine the degree of correlation between E_p and F_{tot}, given that these variables all suffer from some well determined truncation. Below, we present the results of two simulations, using the τ statistic to measure the degree of correlation. Note how well the method recovers the correlation present in the *original* sample, from the *observed* distribution and knowledge of the truncation. (a) In the first case, E_p is from a uniform distribution between 100keV and 2.5MeV, $\alpha = 3.0$, $\beta = -5.0$, the normalization A is from a power law distribution $F(A) \sim A^{0.3}$, and $F_{lim} = 3.0 \times 10^{-9}$. The original, "observed", and corrected correlation results are given in Table A.1. In this case, we have *no* correlation present between E_p and F_{tot} in the original sample, but the truncation produces an artificial correlation in the observed sample, as shown in Figure 7a. Our methods are able to recover the correlation present in the original sample, as seen in Table A.1.

TABLE A.1

Simulation results for the case when truncation produces a correlation.

Variables	Distribution	Number of Bursts	τ
F_{tot} with E_p	Original	1000	0.9σ
F_{tot} with E_p	Observed	490	$> 5.0\sigma$
F_{tot} with E_p	Corrected	490	0.6σ

(b) In the second case, we take the normalization from a power law distribution as in the previous case. The parameter $E_p \sim \xi_i - (A_i/c)^2$, where ξ is some dispersion (a random number between 1 and 100) and c is a constant, α, β, and F_{lim} have the same values as in case (a). Figure 7b shows how the truncation produces a correlation of the opposite sign from the original correlation. Again, the techniques described above were able to quantify this bias, and recover the original correlation. The results for this simulation are given in Table A.2.

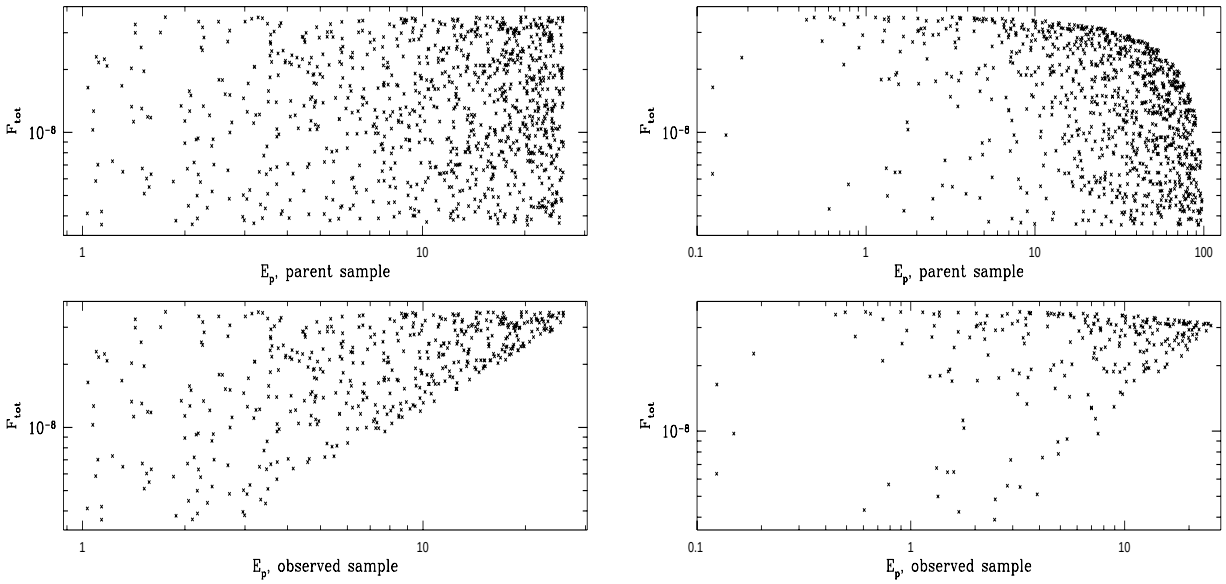

Fig. 7.— **Left Panels:** (a) Total fluence, F_{tot}, vs. peak energy, E_p, for the parent (top panel) and observed (bottom panel) sample for the first simulation in the Appendix. Here, the truncation produces a correlation. **Right Panels:** (b) Same as Figure 7a, for the second simulation given in the Appendix. Here, the truncation produces a correlation of the opposite sign than in the original (parent) sample.

TABLE A.2

Simulation results for the case when truncation changes the sign of the correlation.

Variables	Distribution	Number of Bursts	τ
F_{tot} with E_p	Original	1000	(-) $>5\sigma$
F_{tot} with E_p	Observed	250	(+) 2.5σ
F_{tot} with E_p	Corrected	250	(-) 4.0σ

A.3. Recovering the Functional Form of the Correlation

The method can also be used to recover the *functional dependence* of the correlation present in the original, untruncated sample; this is necessary in understanding the *meaning* of the correlation. Furthermore, once we know the functional dependence, we can remove it from our observed sample to obtain an estimate of the frequency distributions of the relevant variables (see LP99). In this simulation, we begin with a parent sample of 1000 bursts in which $F_{tot} \propto E_p^{1.5}$, with some dispersion. We truncated the sample in a manner described above, to get our observed

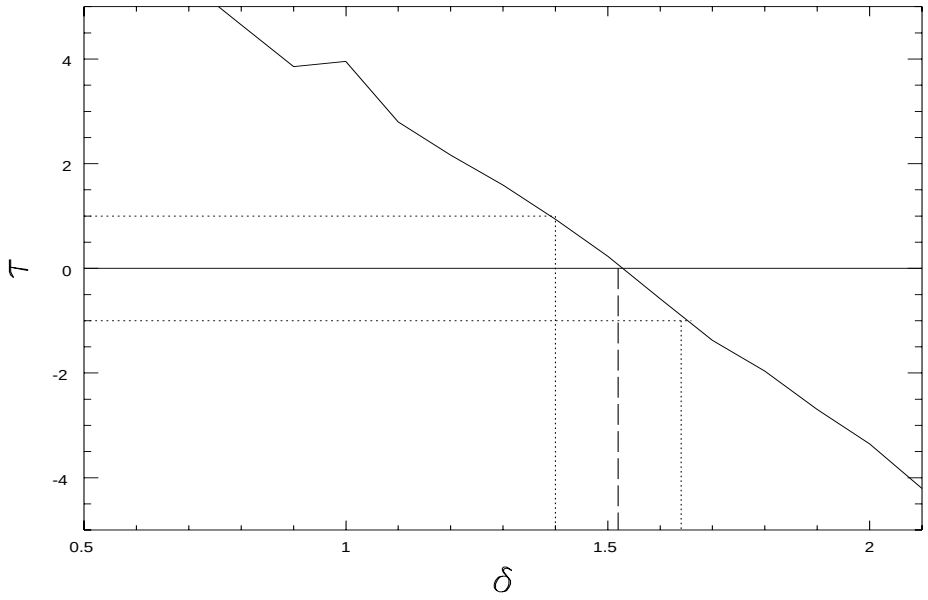

Fig. 8.— Significance of the correlation, τ vs. slope of the power law, δ, describing the functional dependence between F_{tot} and E_p for the "corrected sample", as discussed in §A.3. We recover from the observed sample and knowledge of its truncation, the exact functional dependence present in the parent sample.

sample (170 bursts). We take our observed sample and find the correlation between F_{tot} and E_p, accounting for the limits on E_p and F_{tot}. We then let

$$F_{tot} \longrightarrow F'_{tot} = F_{tot}/q(E_p), \tag{A2}$$

and find the function $q(E_p)$ such that there is no correlation between F'_{tot} and E_p. Our simulations show that the correlation is removed when we let $q(E_{p,i}) \propto E_p^{\delta}$ where $\delta = 1.51 \pm .1$. That is, our methods determine the exact functional form of the correlation present in the parent sample. Figure 8 shows the degree of correlation τ vs. δ in our simulations. The correlation is removed when $\tau = 0$. The vertical lines mark the 1σ confidence intervals. Again, once we have determined the functional form of the correlation, we can remove the correlation to estimate the true frequency distribution of the relevant parameters (LP99).

REFERENCES

Band, D., et al. 1993, ApJ, 413, 281

Bloom, J.S., et al. 1998, ApJ, 507, L25

Brainerd, J.J. 1997, ApJ, 487, 96

Brainerd, J.J., et al. 1999, to appear in the Proceedings of the 20th Texas Symposium on Relativistic Astrophysics, Dec., 1998, Paris, France; also astro-ph 9904039

Dermer, C. D., Chiang, J., Boettcher, M. 1998, ApJ, 513, 656

Djorgovski et al. 1998, ApJ, 508 L17

Djorgovski et al. 1999a GCN Circ. No. 189

Djorgovski et al. 1999b GCN Circ. No. 289

Efron, B. & Petrosian, V. 1992, Ap.J., 399, 345

Efron, B. & Petrosian, V. 1999, Journal of American Statistical Association, in press; also astro-ph 9808334

Galama, T.J. 1999, GCN No. 388

Hakkila, J., et al. 1995, in Gamma Ray Bursts, AIP Conf. Proc. 307, eds. G.J. Fishman, J.J. Brainerd, K.Hurley (New York: AIP), 387

Hjorth, J., et al. 1999 GCN No. 219

Hughes D., et al. 1998, Nature, 394, 291

Kelson et al. 1999, I.A.U.C. 7096

Kulkarni et al. 1998, Nature 393, 35

Lee, T.T. & Petrosian, V. 1996, ApJ, 470, 479

Lee, T.T. & Petrosian, V. 1997, ApJ, 474, L37

Lloyd, N.M. & Petrosian, V. 1999 (LP99), ApJ, 411, 550

Madau, P. 1998, ApJ 498, 106

Mallozzi, R.S., et al. 1995, ApJ, 454, 597

Mallozzi, R.S., et al. 1998, in Gamma Ray Bursts, AIP Conf. Proc. 428, eds. C.A. Meegan, R.D. Preece, T.M. Koshut (New York: AIP), 273

Mallozzi, R.S. et al. 1999, in preparation.

Metzger, M.R. et al. 1997, Nature, 387, 879

Mészáros, P. & Mészáros, A. 1995, ApJ, 449, 9

Mészáros, P., Rees, M.J. 1993, ApJ, 405, 278

Pacholczyk, A.G. 1970, Radio Astrophysics (W.H. Freeman and Company: San Francisco)

Paciesas, W.S. et al. 1999, ApJS, 122, 465

Petrosian, V. 1993, ApJ, 402, L33

Petrosian, V. & Lee, T. 1996, ApJ, 467, L29

Piran, T. 1999, Physics Reports, 314, 575

Rees, M.J. & Mészáros, P. 1992, MNRAS, 258, P41

Rees, M.J. & Mészáros, P. 1994, ApJ, 430, L93

Reichert, D.E. & Mészáros, P. 1997, ApJ, 483, 597

Rutledge, R.E., et al. 1995, MNRAS, 276, 753

Sanders, D.B. 1999, To appear in "Space Infrared Telescopes and Related Science", 32nd COSPAR workshop, Nagoya, Japan 1998, ed. T. Matsumoto, T. de Graauw; also astro-ph 9904292

Sari, R. & Piran, T. 1997, MNRAS, 287, 110

Tavani, M. 1996 ApJ, 466, 768

Vreeswijk, P.M. et al., 1999 GCN No. 324